Revista Mexicana de Astronomía y Astrofísica, **43**, 315–327 (2007)

PHOTOMETRY OF POLAR-RING GALAXIES

Arturo Godínez-Martínez,[1] Alan M. Watson,[1] Lynn D. Matthews,[2] and Linda S. Sparke[3]

Received 2007 May 11; accepted 2007 June 19

RESUMEN

Se obtuvo fotometría en B y R en siete galaxias con anillo polar, probables o confirmadas, del Catálogo de Anillos Polares (PRC) de Whitmore et al. (1990). Los anillos tienen un amplio intervalo de colores de $B-R \approx 0.6$ hasta $B-R \approx 1.7$. Los anillos más azules contienen brillantes regiones H II, las cuales son evidencia directa de formación estelar reciente. La edad mínima del anillo más rojo, el de PRC B-20, es algo incierta debido a la falta de conocimiento del enrojecimiento interno y la metalicidad en este sistema, pero parece ser al menos de 1.2 Gyr. Por lo tanto, este anillo parece ser estable, al menos durante varios periodos rotacionales. Este anillo es un excelente candidato para estudios futuros que podrán determinar de mejor manera si en realidad es un anillo viejo.

ABSTRACT

We have obtained photometry in B and R for seven confirmed or probable polar-ring galaxies from the Polar-Ring Catalog of Whitmore et al. (1990). The rings show a range of colors from $B-R \approx 0.6$ to $B-R \approx 1.7$. The bluest rings have bright H II regions, which are direct evidence for recent star formation. The minimum age of the reddest ring, that in PRC B-20, is somewhat uncertain because of a lack of knowledge of the internal reddening and metallicity, but appears to be at least 1.2 Gyr. As such, this ring is likely to be stable for at least several rotation periods. This ring is an excellent candidate for future studies that might better determine if it is truly old.

Key Words: **GALAXIES: HALOS — GALAXIES: PHOTOMETRY — GALAXIES: STELLAR CONTENT**

1. INTRODUCTION

Polar-Ring Galaxies are systems with two kinematically distinct components (Schechter & Gunn 1978). The central component is an apparently normal galaxy, usually an S0. The second is a ring of gas, dust, and stars whose orbital plane is close to orthogonal to that of the host galaxy. The rings are thought to be the result of an interaction between the host galaxy and a donor (Schweizer, Whitmore, & Rubin 1983).

The ages of the rings are interesting from at least two points of view. First, by combining the mean age of the rings with the current frequency of polar-ring galaxies, once can estimate the frequency with which polar rings are formed. By comparing this to the frequency of all types of interactions, one might hope to learn which kinds of interactions produce polar rings. Second, it is not clear that polar rings are stable. Inclined orbits in a oblate potential suffer differential precession, and so a ring formed by populating such orbits would be smeared out on a few orbital timescales. If rings are long-lived, then it may be that they are self-gravitating or that the halos of the host galaxies are triaxial (see the discussion in Cox & Sparke 1996 and Sparke 2004).

The stars currently seen in the ring almost certainly formed from the gas of the ring (Bournaud & Combes 2003). Therefore, their age sets a lower limit to the age of the ring. The standard means to measure the age of an unresolved stellar population is to interpret broadband photometry using stellar population synthesis methods. A truly old ring should be red, although reddening by dust could disguise a young ring as an old one. Furthermore, the precise mapping from unreddened color to age depends quite

[1]Centro de Radioastronomía y Astrofísica, Universidad Nacional Autónoma de México, Mexico.

[2]Harvard-Smithsonian Center for Astrophysics, USA.

[3]Department of Astronomy, University of Wisconsin-Madison, USA.

TABLE 1

OBSERVING LOG

Galaxy	Coordinates (J2000)	Date	Exposures in $B2$	Exposures in $R2$
PRC A-01, A 0136-0801	01 38 55.2 −07 45 56	2001 September 19	2×1000 s	2×500 s
PRC A-04, UGC 7576	12 27 41.8 +28 41 53	2001 April 26	2×1000 s	2×500 s
PRC A-06, UGC 9796, II Zw 73	15 15 56.3 +43 10 00	2001 April 24 and 30	4×1000 s	4×500 s
PRC B-10, A 0950-2234	09 52 53.9 −22 48 34	2001 April 26 and 29	4×1000 s	4×500 s
PRC B-17, UGC 9562, II Zw 71	14 51 14.4 +35 32 32	2001 April 24	2×1000 s	2×500 s
PRC B-20, A 2135-2132	21 38 20.0 −21 19 06	2001 September 20	2×1000 s	2×500 s
PRC B-21, ESO 603-G21	22 51 22.0 −20 14 50	2001 September 19	2×1000 s	2×500 s

sensitively on the metallicity and star-formation history.

Many polar rings are quite blue (see § 5.2) and are not good candidates for old rings. Our aims in this work are to attempt to identify red rings using $B - R$ photometry. We selected $B - R$ as a good compromise between sensitivity and color information. Because of the uncertainties introduced by dust, metallicity, and star-formation history, we do not pretend to be able to extract precise ages on the basis of a single color. However, red rings are excellent candidate subjects for future investigations to confirm whether they are indeed old rings.

2. OBSERVATIONS

We observed seven polar-ring galaxies from the Polar Ring Catalog (Whitmore et al. 1990) using the 1.5-m telescope of the Observatorio Astronómico Nacional on Sierra San Pedro Mártir, Baja California, México, the SITe1 1024×1024 CCD (binned 2×2 to give a scale of $0\farcs51$/pixel and a field of view of $4\farcm3$) and the $B2$ (1 mm CG285 + 1 mm BG18 + 2 mm BG12) and $R2$ (2 mm KG3 + 2 mm OG570) filters. Table 1 gives names and equatorial coordinates of each galaxy (from NED) and the dates and exposure times of the observations. We obtained bias and twilight flat field exposures each night.

We used IRAF to reduce the exposures of the galaxies. Specifically, we used the ccdred package to construct and apply bias and flat field corrections, the cosmicrays task to identify automatically and interpolate automatically over cosmic ray events, and the imedit task to interpolate manually over remaining cosmic ray events. We shifted the exposures in each filter into a common alignment and summed them. The first columns of Figures 1 to 7 show the final images of each galaxy in $B2$ and $R2$.

The galaxies were observed in the course of observing runs in the spring and fall of 2001 on the 1.5-meter telescope. After the fall run on the 1.5-meter telescope, we had a run on the adjacent 84-centimeter telescope with the same SITe 1 CCD and the same $B2$ and $R2$ filters. During these three runs we observed photometric standards from Landolt (1983). Subsequent analysis showed that nine nights on the 1.5-meter telescope and a further two nights on 84-centimeter telescope were photometric. During these photometric nights we observed a total of 106 (in B) and 107 (in R) photometric standards with $B - R$ colors from -0.4 to $+2.2$ at airmasses from 1.1 to 2.3. We reduced the standards in the same way as the galaxies, except that we did not interpolate manually over cosmic ray events.

We performed aperture photometry on the standard stars using the apphot package. We used an aperture of diameter $15\farcs2$. We fitted for the transformation from instrumental to standard magnitudes, allowing for a zero point, a linear extinction term, and a linear color term. We fitted for different zero points and extinction coefficients for each night but for a single color coefficient for the whole set of nights. Using a single color coefficient improves the precision of the fit. (This is the reason for including data from the 84 centimeter telescope, even though we observed no galaxies during this run.) The RMS residuals were 2.0% in B and 1.3% in R. The extinction coefficients varied between 0.17 and 0.32 for $B2$ and 0.07 and 0.17 in $R2$.

The transformations from the natural $B2$ and $R2$ magnitudes to the standard B and R magnitude were $B = B2 + 0.112(B - R)$ and $R = R2 + 0.008(B - R)$. This indicates that the $B2$ and $R2$ bandpasses are redder than the standard bandpasses, with $B2$ being redder by about 200 Å. Given that the $B2$ filter is constructed according to a recipe for photocathodes rather than CCDs, these differences are not surprising.

3. MODEL FITTING

Polar rings are often faint compared to their host galaxies. For this reason, we modelled and sub-

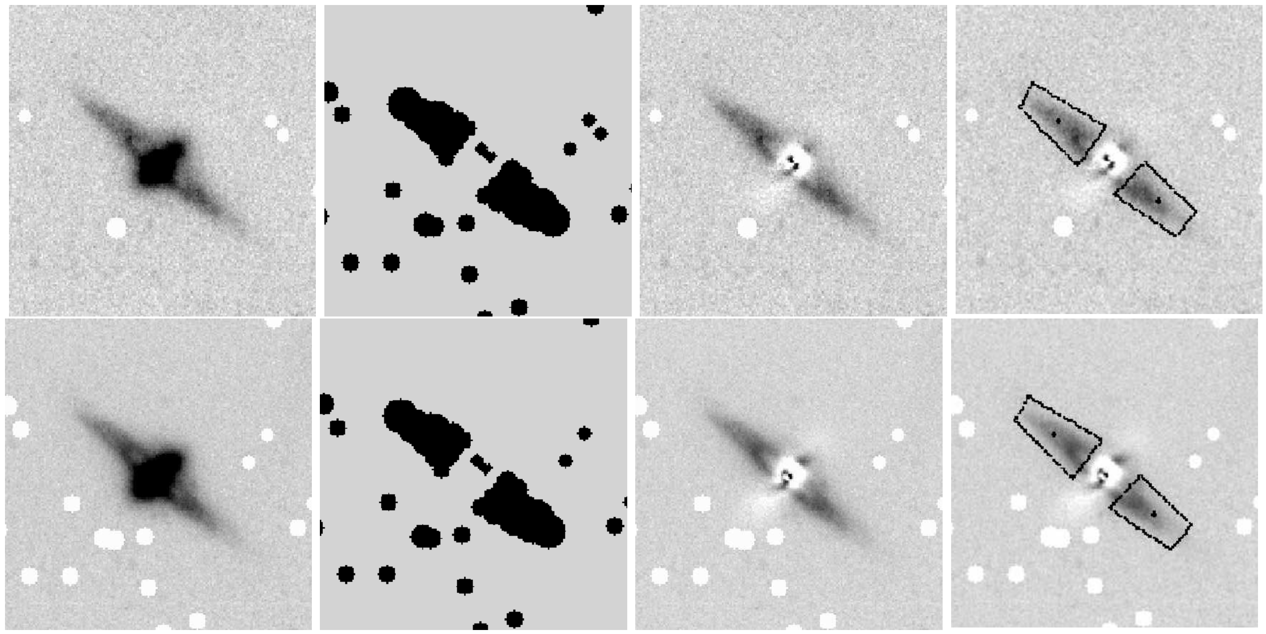

Fig. 1. Images of PRC A-01 in $B2$ (top row) and $R2$ (bottom row). The images are $90'' \times 90''$. North is up and east is left. The first column shows the host galaxy and the ring. The second column shows the mask used to discard certain regions from the model fit to the host galaxy. The third column shows the ring after the model of the host galaxy is subtracted. The fourth column shows the apertures used for photometry of the ring.

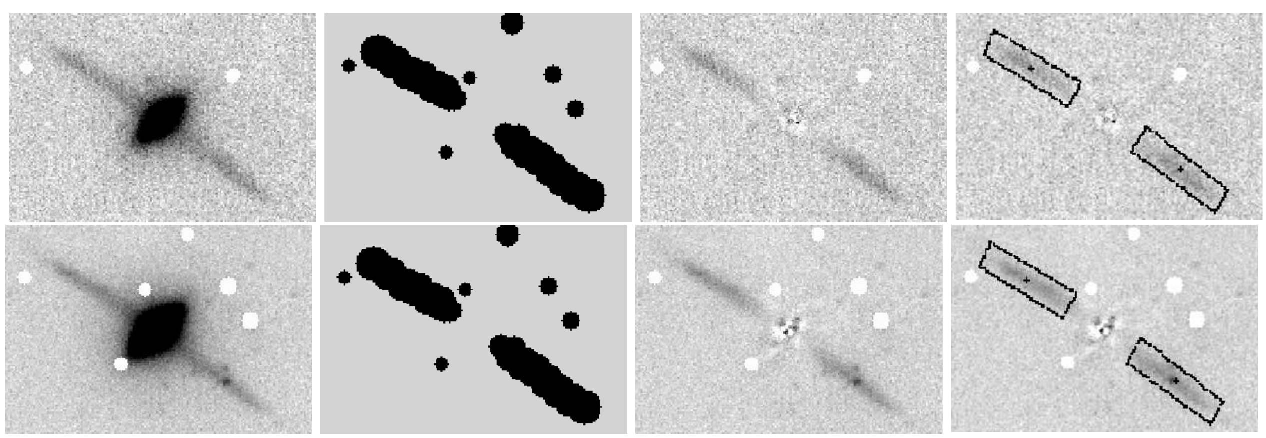

Fig. 2. Images of PRC A-04 in $B2$ (top row) and $R2$ (bottom row). The images are $90'' \times 60''$. Otherwise as Figure 1.

tracted the host galaxies to allow for better photometry of the rings.

We fitted models to the galaxies using Galfit (Peng et al. 2002). This program takes an image, an uncertainty image, and a point-spread function (PSF) image and fits a model consisting of a tilted plane for the sky and combinations of Sérsic profiles, exponential disks, Gaussians, and PSFs for the galaxy. The model parameters are adjusted to minimize the reduced χ^2_ν.

We began by creating a mask for each image to indicate regions that should not be included in the fit. These regions include stars, the brightest parts of the ring, and the region in the galaxy PRC A-01 where the near side of the ring passes over the galaxy and causes significant extinction. The second columns of Figures 1 to 7 show these masks. We created PSF images using field stars and uncertainty images using the known gain and read noise of the CCD.

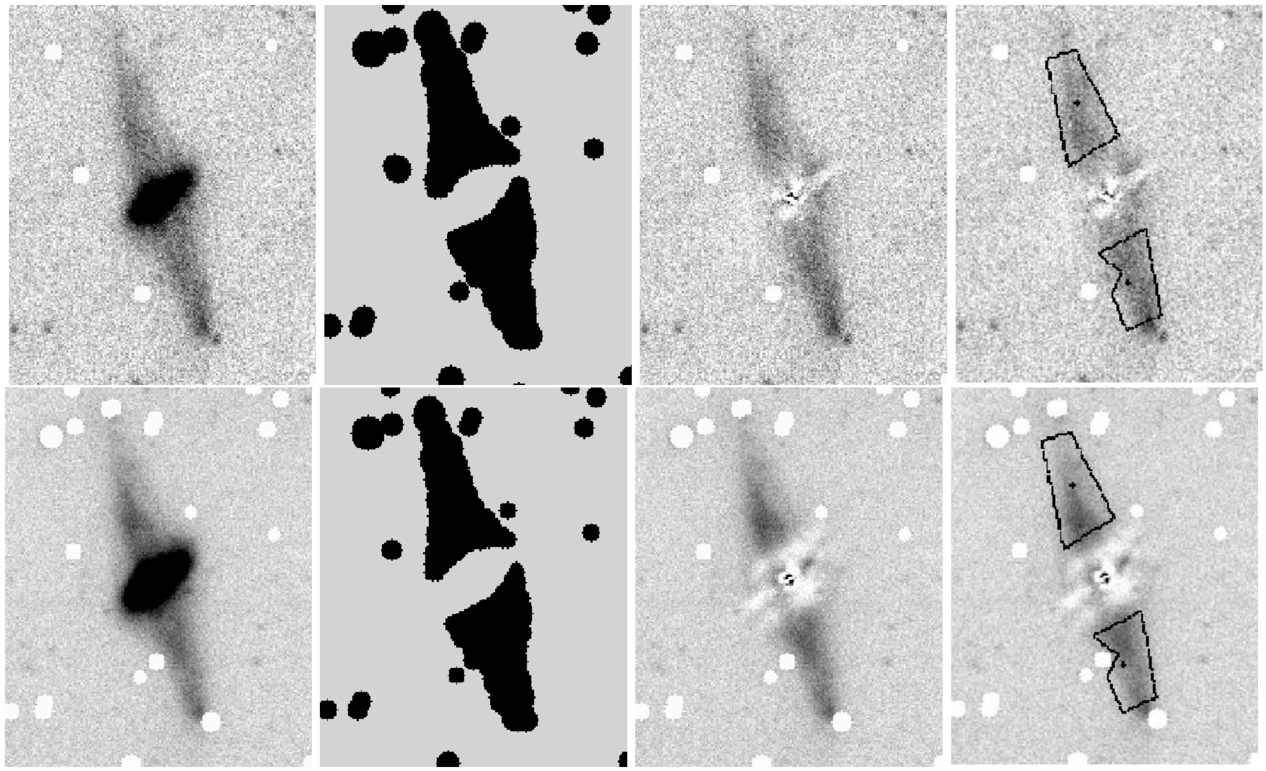

Fig. 3. Images of PRC A-06 in $B2$ (top row) and $R2$ (bottom row). The images are $90'' \times 110''$. Otherwise as Figure 1.

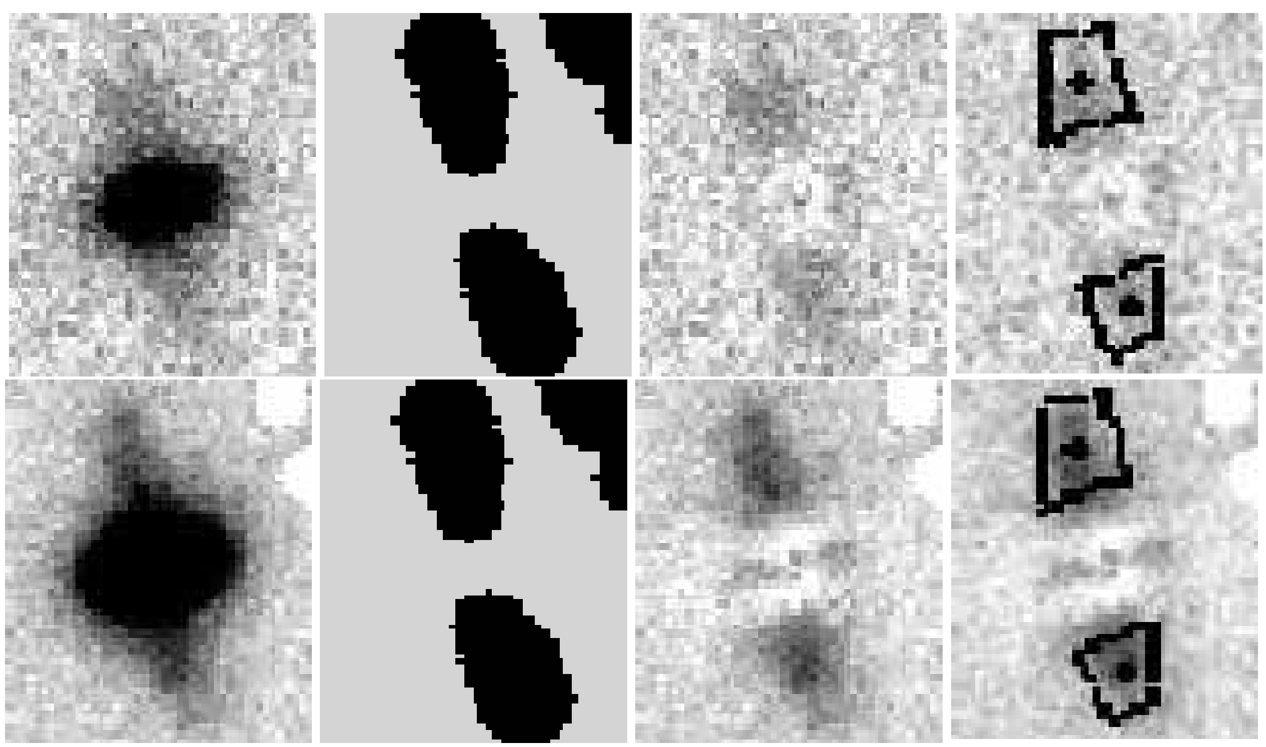

Fig. 4. Images of PRC B-10 in $B2$ (top row) and $R2$ (bottom row). The images are $21'' \times 25''$. Otherwise as Figure 1.

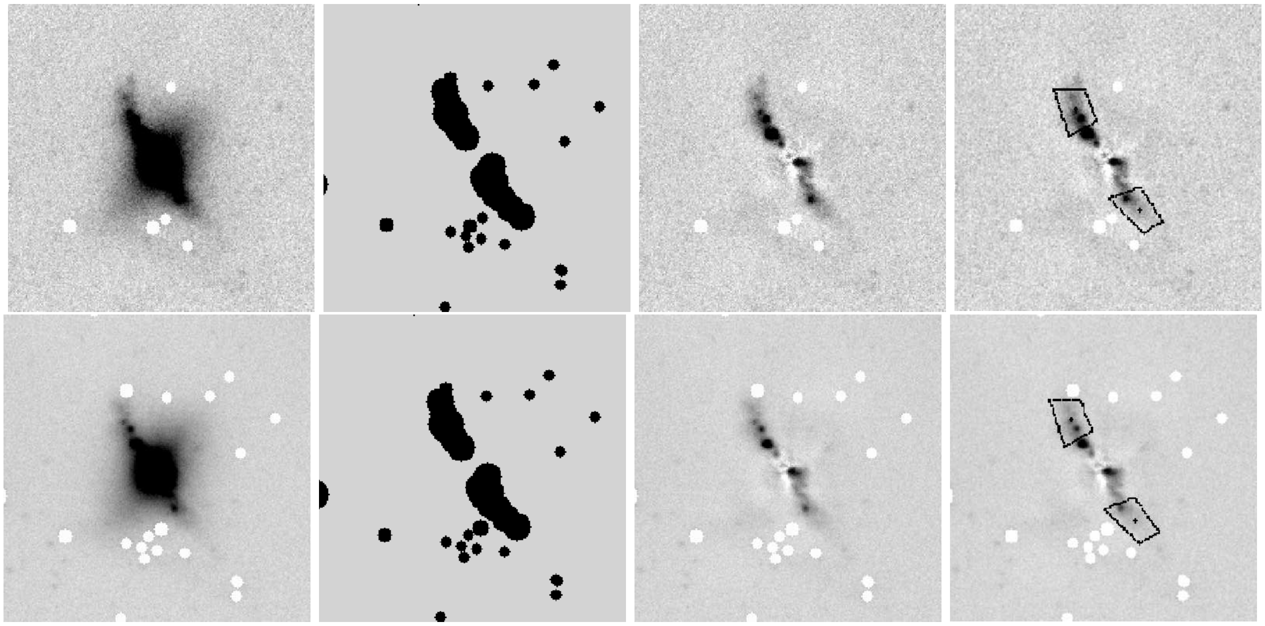

Fig. 5. Images of PRC B-17 in $B2$ (top row) and $R2$ (bottom row). The images are $110'' \times 110''$. Otherwise as Figure 1.

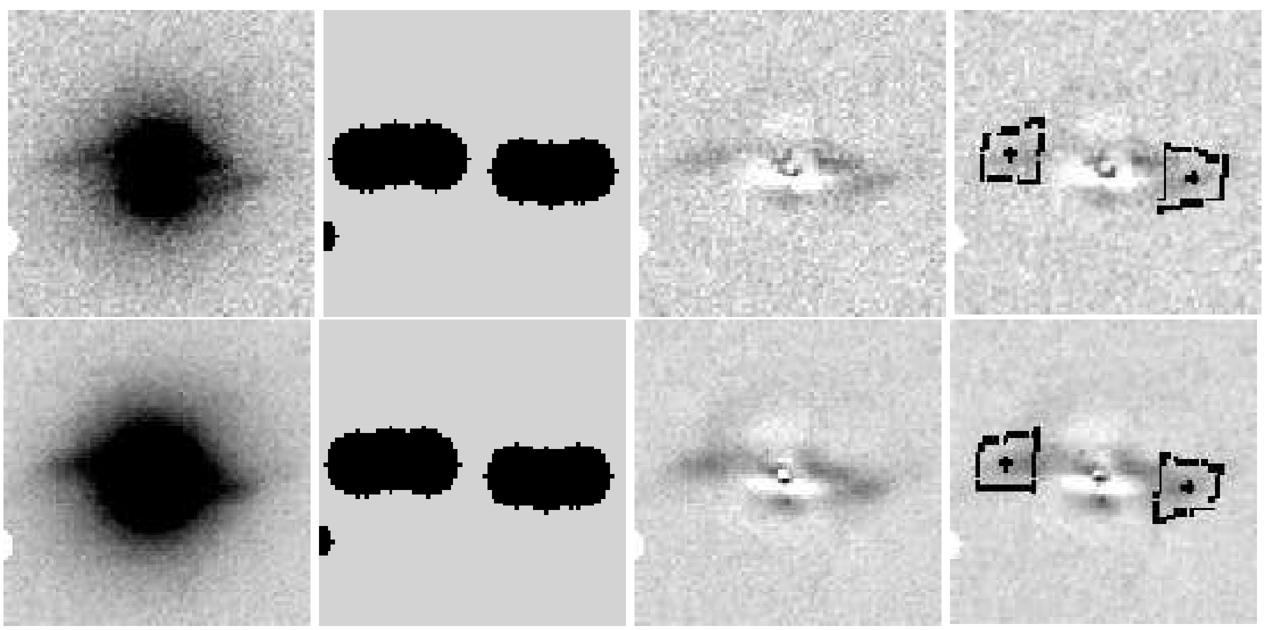

Fig. 6. Images of PRC B-20 in $B2$ (top row) and $R2$ (bottom row). The images are $37'' \times 37''$. Otherwise as Figure 1.

We began modelling the galaxies with a tilted plane for the sky and a single Sérsic or exponential disk component. We added components until the reduced χ^2_ν of the fit no longer decreased significantly. The components are listed in Table 2. See Peng et al. (2002) for definitions of the fitted components and their parameters. The third columns of Figures 1 to 7 show the images after subtracting the models of the host galaxy.

Some of the components have clear physical interpretations, but others, especially the Gaussians, do not. We suspect that such ad hoc components appear because of errors in the PSF, dust absorption close to the center of the galaxies, and because the

TABLE 2

FITTED COMPONENTS

Galaxy	Filter χ^2_ν	Component	$\Delta\alpha$[a]	$\Delta\delta$[a]	Δm[b]	r[c]	n[d]	q[e]	PA[f]	c[g]
PRC A-01	B	Sérsic	$0\farcs0$	$0\farcs0$	0.00	$4\farcs9$	1.20	0.59	−44.3	−0.32
	1.5	PSF	$-0\farcs9$	$+0\farcs9$	1.34	...	...	...	...	...
		Gaussian	$-0\farcs3$	$-0\farcs3$	3.08	$0\farcs3$	...	0.04	−22.8	−1.76
	R	Sérsic	$0\farcs0$	$0\farcs0$	0.00	$4\farcs8$	1.39	0.55	−44.7	−0.21
	2.0	Gaussian	$-0\farcs4$	$+0\farcs5$	1.19	$1\farcs5$	...	0.30	+14.0	−0.86
		PSF	$-0\farcs9$	$-0\farcs2$	4.61	...	...	...	...	...
PRC A-04	B	Sérsic	$0\farcs0$	$0\farcs0$	0.00	$12\farcs6$	1.16	0.79	+61.3	−0.64
	1.3	Sérsic	$+0\farcs2$	$-0\farcs8$	0.47	$5\farcs5$	0.78	0.27	−46.8	+1.05
		Sérsic	$-0\farcs1$	$-0\farcs5$	0.95	$1\farcs4$	1.66	0.59	−9.6	−1.25
	R	Sérsic	$0\farcs0$	$0\farcs0$	0.00	$10\farcs2$	1.76	0.89	−53.8	−0.22
	1.2	Sérsic	$+0\farcs2$	$-0\farcs2$	0.79	$5\farcs7$	0.57	0.29	−45.7	−0.04
		Sérsic	$+0\farcs1$	$-0\farcs1$	1.13	$0\farcs8$	1.41	0.08	−25.8	0.00
		PSF	$-0\farcs3$	$+2\farcs0$	4.75	...	...	...	...	...
PRC A-06	B	Sérsic	$0\farcs0$	$0\farcs0$	0.00	$7\farcs4$	1.35	0.67	−33.2	−0.12
	1.8	Sérsic	$-2\farcs9$	$+1\farcs8$	0.83	$7\farcs3$	0.37	0.22	−55.2	0.00
		Sérsic	$-1\farcs8$	$+1\farcs2$	1.40	$1\farcs3$	0.03	0.82	+77.2	−0.51
		PSF	$-2\farcs4$	$+1\farcs4$	2.05	...	...	...	...	...
	R	Sérsic	$0\farcs0$	$0\farcs0$	0.00	$5\farcs6$	0.83	0.27	−54.5	0.00
	1.4	Sérsic	$-0\farcs9$	$+0\farcs6$	0.36	$10\farcs7$	0.24	0.65	−30.4	−0.71
		Sérsic	$+0\farcs0$	$+0\farcs4$	1.23	$1\farcs1$	0.88	1.00	−70.2	−0.72
		PSF	$-0\farcs8$	$+0\farcs4$	1.47	...	...	...	...	...
PRC B-10	B	Sérsic	$0\farcs0$	$0\farcs0$	0.00	$3\farcs2$	1.79	0.59	−75.7	+0.06
	1.1									
	R	Sérsic	$0\farcs0$	$0\farcs0$	0.00	$3\farcs2$	1.18	0.57	−76.4	+0.43
	1.0	PSF	$-0\farcs2$	$+0\farcs0$	2.15	...	...	...	...	...
PRC B-17	B	Sérsic	$0\farcs0$	$0\farcs0$	0.00	$13\farcs1$	1.70	0.46	+34.1	+0.16
	1.8	Exp.	$+0\farcs5$	$+0\farcs9$	0.07	$10\farcs2$	...	0.50	−37.7	−0.20
		Sérsic	$+0\farcs3$	$+1\farcs8$	2.62	$1\farcs4$	1.20	0.75	−79.6	−0.42
	R	Exp.	$0\farcs0$	$0\farcs0$	0.00	$9\farcs6$	...	0.57	−37.7	−0.34
	1.2	Sérsic	$+0\farcs3$	$-1\farcs0$	0.52	$10\farcs3$	1.59	0.54	+30.2	+0.60
		Sérsic	$+0\farcs2$	$+0\farcs8$	3.02	$1\farcs6$	2.07	0.74	−67.7	−0.56
PRC B-20	B	Exp.	$0\farcs0$	$0\farcs0$	0.00	$5\farcs3$	...	0.92	−63.6	−0.14
	1.2	Sérsic	$-0\farcs6$	$+0\farcs2$	1.40	$2\farcs9$	0.72	0.61	+4.7	+0.70
		PSF	$-0\farcs4$	$+0\farcs1$	2.68	...	...	...	...	...
	R	Exp.	$0\farcs0$	$0\farcs0$	0.00	$5\farcs3$	...	0.91	−68.2	−0.12
	1.6	Sérsic	$-0\farcs2$	$+0\farcs2$	0.96	$2\farcs5$	1.34	0.64	+8.8	+0.55
		PSF	$-0\farcs2$	$+0\farcs3$	2.60	...	...	...	...	...
PRC B-21	B	Sérsic	$0\farcs0$	$0\farcs0$	0.00	$8\farcs2$	0.37	0.97	+65.9	+0.77
	1.6	Sérsic	$+1\farcs9$	$+1\farcs8$	2.36	$2\farcs8$	0.32	0.67	−63.1	−0.18
	R	Sérsic	$0\farcs0$	$0\farcs0$	0.00	$7\farcs3$	0.47	0.96	+70.4	+0.89
	2.3	Sérsic	$+0\farcs9$	$+0\farcs6$	2.39	$2\farcs1$	0.68	0.42	−64.6	+0.50

[a]Offsets between the centers of the components.

[b]Magnitude relative to the brightest component (which has $\Delta m \equiv 0$).

[c]r is r_e for exponenential profiles, r_s for Sérsic profiles, and FWHM for Gaussian profiles.

[d]$1/n$ is the Sérsic profile exponent.

[e]q is the axis ratio.

[f]PA is the position angle.

[g]c is the *diskiness* (positive) or *boxiness* (negative) parameter.

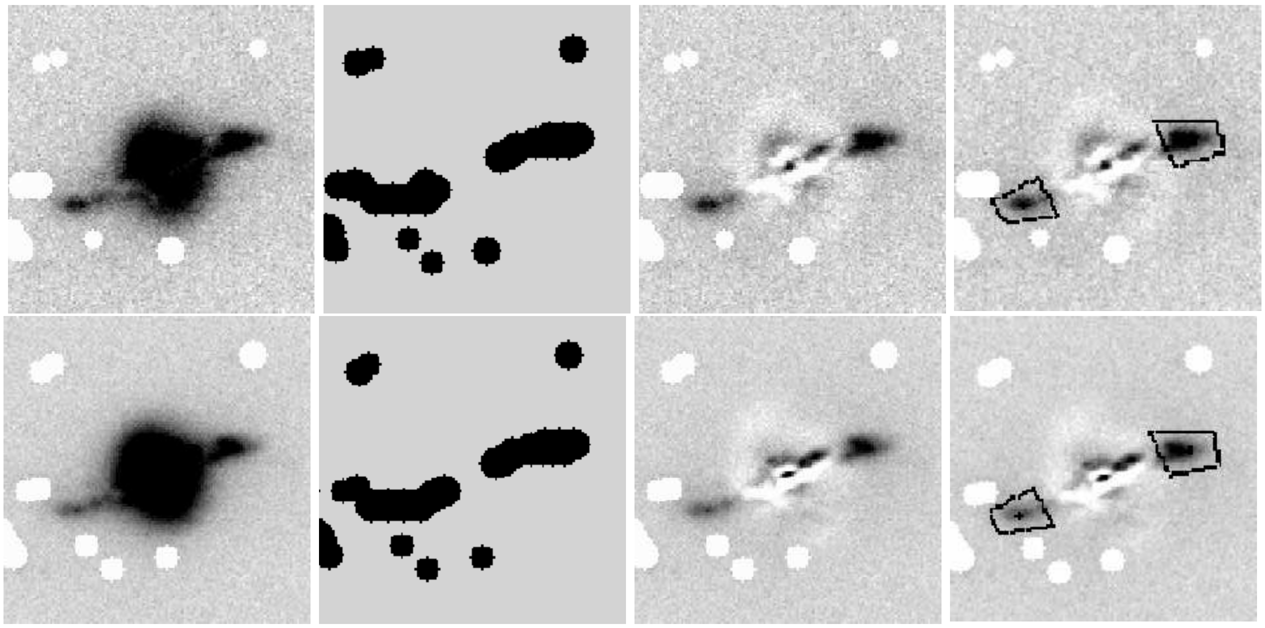

Fig. 7. Images of PRC B-21 in $B2$ (top row) and $R2$ (bottom row). The images are $65'' \times 65''$. Otherwise as Figure 1.

TABLE 3

ASSUMED GALACTIC EXTINCTION

Galaxy	A_{B2}	A_{R2}
PRC A-01	0.110	0.071
PRC A-04	0.089	0.058
PRC A-06	0.110	0.072
PRC B-10	0.192	0.124
PRC B-17	0.052	0.034
PRC B-20	0.178	0.116
PRC B-21	0.137	0.089

components in Galfit are more appropriate for fitting less inclined galaxies. Nevertheless, we are not especially worried by this as our aim is not to investigate the structure of the host galaxies but simply to remove their light. Also, despite our attempts to exclude the rings from the fits, the models often seem to remove the rings where they are projected against the host galaxy. For these reasons we will restrict our photometry of rings to the parts that are not projected over bright regions the host galaxy.

4. PHOTOMETRY

4.1. *Galactic Extinction*

We correct our photometry for Galactic extinction using values from NED, which are taken from appendix B of Schlegel, Finkbeiner, & Davis (1998). Extinction corrections must be calculated for the wavelengths of the natural system. Since our $R2$ filter is very similar to the the standard R, we use $A_{R2} = A_R$. However, since our $B2$ bandpass is about 200 Å redder than the standard bandpass, we use $A_{B2} = 0.8A_B + 0.2A_V$. Table 3 lists are adopted extinction values. The largest reddening is 0.07 for PRC B-10.

4.2. *Host Galaxies*

The host galaxies are not the focus of this work. Nevertheless, we obtained photometry of the host galaxies primarily to permit a comparison of our photometry with previous photometry (see § 4.4).

We obtained photometry for the host galaxies both from aperture photometry and from the Galfit models. For the aperture photometry, we first subtracted the sky as determined by Galfit and then used the apphot package with apertures of diameter $15\farcs2$, identical to those used for our standard stars, with the background fixed at zero. For the model photometry, we summed the components fitted by Galfit. Table 4 shows the extinction-corrected R_0 magnitudes and $(B-R)_0$ colors for both methods. The model colors are similar or slightly bluer than the aperture colors; this may reflect color gradients in some of the galaxies.

We estimated uncertainties for our aperture photometry taking into account the contribution of uncertainties in the calibration (2.0% in B and 1.4% in

TABLE 4

PHOTOMETRY

Galaxy	Aperture[a]		Model[b]		Ring[c]	
	R_0	$(B-R)_0$	R_0	$(B-R)_0$	R_0	$(B-R)_0$
PRC A-01	14.62 ± 0.01	$+1.62 \pm 0.02$	14.44	+1.62	16.23 ± 0.03	$+1.21 \pm 0.05$
PRC A-04	14.72 ± 0.01	$+1.57 \pm 0.03$	14.23	+1.53	17.35 ± 0.07	$+1.10 \pm 0.15$
PRC A-06	14.96 ± 0.01	$+1.59 \pm 0.02$	14.66	+1.53	16.58 ± 0.03	$+1.07 \pm 0.06$
PRC B-10	16.14 ± 0.02	$+1.65 \pm 0.05$	16.16	+1.58	18.73 ± 0.04	$+1.49 \pm 0.16$
PRC B-17	14.71 ± 0.01	$+0.89 \pm 0.03$	13.69	+0.86	16.97 ± 0.04	$+0.61 \pm 0.06$
PRC B-20	14.68 ± 0.01	$+1.78 \pm 0.03$	14.18	+1.67	18.45 ± 0.03	$+1.67 \pm 0.10$
PRC B-21	14.87 ± 0.01	$+1.77 \pm 0.03$	14.22	+1.60	17.00 ± 0.02	$+0.89 \pm 0.04$

[a]Photometry in $15\farcs2$ diameter circular aperture.

[b]Photometry from Galfit.

[c]Photometry in polygonal apertures over the ring. Note that these apertures do not cover the whole ring and so the magnitudes given here underestimate the total ring magnitude.

R), Poisson noise in the object and sky, uncertainties in the flat field, and uncertainties in the determination of the sky level. We estimated the later two by measuring the sky in about a dozen small regions isolated from the galaxy and other sources such as stars and calculating the standard deviation between these sky measurements. In all galaxies except PRC B-10 in B, the dominant contributor to the noise is the uncertainty in the calibration. In B-10 in B, the dominant contributor is uncertainty in the determination of the sky level.

We have not calculated uncertainties for our photometry of the models because the model photometry is peripheral to our aims here, and because obtaining uncertainties for the model parameters is involved. Nevertheless, we expect them to be similar to the uncertainties in our aperture photometry.

4.3. *Polar Rings*

To measure the ring colors, we obtained aperture photometry of the rings over regions uncontaminated by the host galaxy. We used the images after subtracting the sky and model determined by Galfit. We defined polygonal apertures on the brightest and most isolated parts of the ring and used the polyphot task in the apphot package with the background fixed at zero. Table 5 lists the offsets west and north from the center of the galaxies of the vertices of the apertures. Table 4 shows the ring aperture magnitudes and colors corrected for Galactic extinction.

We estimated the uncertainties in the same way as for the aperture photometry of the host galaxies. In all cases the dominant contributor is uncertainty in the determination of the sky level.

Galfit can fit the sky using a tilted plane, which provides a clear improvement over a simple constant. For example, if we had used a constant rather than a tilted plane, our uncertainty in the $B-R$ color of the ring of PRC B-20 would have been 0.34 rather than 0.10. Furthermore, our use of polygonal apertures rather than circular apertures allowed us to reduce the uncertainty associated with the sky level. Reshetnikov, Hagen-Thorn, & Yakovleva (1994) used a pair of 40 $''$ diameter apertures for their photometry of the ring of PRC A-06. These apertures have a combined area that is about 3.5 times larger than our apertures. If we had used these apertures, our uncertainty in the $B-R$ color of the ring of PRC A-06 would have been 0.21 rather than 0.06.

4.4. *Approximate Color Transformations*

We are faced with the problem that different authors measure different colors. To facilitate comparison, we have converted other colors to $B-R$ using the approximate transformations

$$(B-R) \approx 1.60 \pm 0.03(B-V), \quad (1)$$

$$(B-R) \approx 1.29 \pm 0.07(V-I), \quad (2)$$

$$(B-R) \approx 0.71 \pm 0.02(B-I). \quad (3)$$

The coefficients are the mean coefficients for populations with ages of 10^9, 5×10^9, and 10^{10} years and metallicities Z of 0.004, 0.008, 0.02, and 0.05 according to the models of Kurth, Fritze-v. Alvensleben, & Fricke (1999). We also show the dispersion of the 12 individual coefficients around these

TABLE 5

OFFSETS OF THE VERTICES OF THE RING PHOTOMETRY APERTURES

Galaxy	Vertices (West, North)
PRC A-01	$(-1''.0, +10''.0), (-9''.6, -1''.6), (-26''.8, +15''.6), (-22''.8, +22''.7)$ $(+10''.5, -0''.6), (+1''.4, -10''.2), (+19''.6, -22''.3), (+25''.7, -15''.3)$
PRC A-04	$(-8''.5, +10''.0), (-12''.5, +2''.9), (-37''.3, +18''.1), (-34''.3, +25''.2)$ $(+10''.6, -2''.9), (+6''.6, -10''.5), (+31''.4, -28''.2), (+34''.9, -21''.6)$
PRC A-06	$(+3''.1, +17''.1), (-12''.1, +8''.0), (-18''.6, +39''.9), (-10''.0, +42''.4)$ $(-3''.3, -17''.6), (+10''.9, -10''.6), (+15''.5, -35''.9), (+5''.3, -40''.4), (+0''.8, -29''.8), (+3''.8, -23''.2)$
PRC B-10	$(+1''.6, +5''.6), (-4''.4, +3''.6), (-4''.4, +11''.2), (-0''.4, +11''.7)$ $(-1''.9, -6''.5), (+3''.1, -4''.5), (+3''.1, -10''.1), (+0''.1, -11''.6)$
PRC B-17	$(-3''.7, +13''.4), (-13''.8, +7''.8), (-19''.4, +25''.0), (-8''.3, +25''.0)$ $(+0''.6, -14''.9), (+11''.7, -10''.8), (+20''.3, -23''.5), (+13''.3, -27''.5)$
PRC B-20	$(-8''.7, -2''.2), (-15''.8, -1''.7), (-15''.3, +3''.3), (-8''.2, +4''.8)$ $(+6''.2, -6''.0), (+7''.2, +2''.1), (+14''.3, +0''.5), (+13''.3, -4''.5)$
PRC B-21	$(-10''.8, -12''.2), (-22''.5, -13''.7), (-25''.0, -9''.2), (-15''.4, -4''.1)$ $(+14''.2, -1''.6), (+9''.7, +8''.0), (+23''.3, +8''.0), (+24''.9, +0''.9)$

mean coefficients. These approximate transformations are appropriate for populations dominated by intermediate-age and old stars.

4.5. *Comparison with Previous Galaxy Photometry*

Table 6 compares our photometry for the host galaxies with that of previous authors. Comparing galaxy colors directly is made difficult by the fact that different workers have used different measurement apertures. Because galaxies often show intrinsic radial color gradients, this can lead to differences in the measured aperture colors at the tenth of a magnitude level. However, we can make a direct comparison of our photometry with that of Mould, Balick, & Aaronson (1982) and Reshetnikov et al. (1994) for PRC A-04. These authors give $B-R$ colors of +1.75 and +1.77 in a $8''.4$ diameter aperture. We measure a color of $+1.66 \pm 0.03$ in this aperture. Unfortunately, the other authors do not give any indications of the likely uncertainties in their measurements, and this makes it impossible to evaluate the difference of about 0.1 magnitudes between our measurement and their measurements. However, if their measurements have similar errors to our measurement, then the difference is only about 2σ and as such is not significant.

Our color for B-17 is consistent with the somewhat uncertain color given by Gil de Paz, Madore, & Pevunova (2003). Our color is slightly bluer than that +0.99 (corrected for Galactic extinction) given by Cox et al. (2001). However, their color was measured on patches of the galaxy away from the ring, whereas our color includes contamination from the bluer ring.

The two worst differences are A-01 and B-21. In the case of A-01 our $B-R$ color is 0.3 magnitudes redder than would be expected from the B and g photometry of Whitmore et al. (1990) converted to $B-V$ by Reshetnikov et al. (1994) and finally to $B-R$ using the approximate transformations above. Interestingly, we both measure the ring to be about 0.4 magnitudes bluer than the host galaxy, which might suggest a problem with the photometic calibration. Unfortunately, Whitmore et al. (1990) give no details of their photometric calibration, instead refering the reader Whitmore, McElroy, & Schweizer (1987). In that paper, the authors use mean extinction coefficients, although it seems unlikely that this could explain all of the difference.

In the case of B-21, our model $B-R$ color is fully 0.7 magnitudes redder than the $B-R$ color measured by Reshetnikov, Fandez-Abans, & Oliveira-Abans (2002), but is in good agreement with the color given by Lauberts & Valentijn (1989) and in reasonable agreement with the color given by Stockton & MacKenty (1983). Reshetnikov et al. (2002) measure similar colors for the host galaxy and the ring, but we measure much bluer colors for the ring.

TABLE 6

COMPARISON OF HOST GALAXY $(B-R)_0$ COLORS

Galaxy	Our Aperture	Our Model	Others
PRC A-01	$+1.61 \pm 0.03$	+1.61	+1.3[ab]
PRC A-02	···	···	+1.6[ac],+1.4[ac]
PRC A-03	···	···	+1.4[ad]
PRC A-04	$+1.57 \pm 0.03$	+1.53	+1.75[e],+1.77[f],+1.30[g]
PRC A-05	···	···	+1.3[ah],+1.4[ai]
PRC A-06	$+1.58 \pm 0.03$	+1.52	+1.47[j]
PRC B-03	···	···	+1.39[k]
PRC B-10	$+1.63 \pm 0.05$	+1.56	···
PRC B-17	$+0.88 \pm 0.03$	+0.85	+0.99[l], $+0.9 \pm 0.2$[m]
PRC B-19	···	···	+1.6[n]
PRC B-20	$+1.76 \pm 0.03$	+1.65	···
PRC B-21	$+1.76 \pm 0.03$	+1.59	+1.4[o],$+1.5 \pm 0.2$[p], 0.90 ± 0.1[q]
PRC C-02	···	···	+0.90[r]
PRC C-03	···	···	+1.31[s]
PRC C-12	···	···	+0.95[r]
PRC C-13	···	···	+2.3[at]
PRC C-27	···	···	+0.73[r]

[a]Color converted to $B-R$ using the approximate transformations of § 4.4. The details of the conversions are mentioned in the notes below.

[b]Reshetnikov et al. (1994), converted from $B-V=+0.8$ obtained in turn by these authors by converting the $B-g$ and $B-i$ colors of Whitmore et al. (1990).

[c]Whitmore et al. (1987), converted from $B-V=1.02\pm0.03$ in an aperture of $2''.9$ over the nucleus and $B-V=0.90\pm0.08$ in the halo.

[d]Peletier & Christodoulou (1993), converted from $B-V=0.87$ outside the central $4''.0$.

[e]Mould et al. (1982), in an aperture of $8''.4$ diameter.

[f]Reshetnikov et al. (1994), in an aperture of $8''.4$ diameter.

[g]Reshetnikov et al. (1994), total magnitude.

[h]Whitmore et al. (1987), converted from $B-V=+0.81$ obtained in turn by these authors from Sérsic & Agüero (1972).

[i]Gallagher et al. (2002), converted from $B-I=2.0$.

[j]Reshetnikov et al. (1994).

[k]Reshetnikov, Hagen-Thorn, & Yakovleva (1995).

[l]Cox et al. (2001).

[m]Gil de Paz et al. (2003).

[n]Peletier et al. (1990).

[o]Stockton & MacKenty (1983).

[p]Lauberts & Valentijn (1989).

[q]Reshetnikov et al. (2002).

[r]Reshetnikov (2004).

[s]Reshetnikov et al. (2005), using an aperture of $20''.0$ diameter.

[t]van Driel et al. (1995), converted from $V-I=+1.8$.

We conclude that the photometry of Reshetnikov et al. (2002) is probably in error. We note again these authors used mean extinction coefficients, although again this is unlikely to lead to an error as large as 0.7 magnitudes.

We conclude that our colors are consistent with previous authors to around one tenth of a magnitude or better, with the exception of the colors of A-01 and B-21 measured by Whitmore et al. (1990) and Reshetnikov et al. (2002). We believe that the internal dispersion in our photometric standards of 0.024 magnitudes in $B-R$ is a reliable reflection of the accuracy of our photometic calibration.

4.6. *Comparison with Previous Ring Colors*

Table 7 compares our photometry for the rings with that of previous authors. We are in good agreement with previous authors on the colors of PRC A-04 and B-17 and reasonable agreement with previous authors on the colors of A-06. We note that for their photometry of A-06, Reshetnikov et al. (1994) used much larger apertures than we have used, and as such their colors may be more sensitive to uncertainties in the determination of the sky level. Our colors for A-01 and B-21 are significantly redder than the colors given by Reshetnikov et al. (1994) and Reshetnikov et al. (2002), but since our photometry of the host galaxy is also different, this is no surprise.

TABLE 7

COMPARISON OF RING COLORS

Galaxy	Our $(B-R)_0$	Others $(B-R)_0$
PRC A-01	$+1.20 \pm 0.05$	$+0.9$[ab]
PRC A-02	···	$+1.0$[ac]
PRC A-03	···	$+1.1$[ad]
PRC A-04	$+1.10 \pm 0.15$	$+0.82$[e], $+1.0 \pm 0.1$[f]
PRC A-05	···	-0.1[ag],$+1.1$[ah]
PRC A-06	$+1.07 \pm 0.06$	$+0.91$[i]
PRC B-03	···	$+0.6 \pm 0.14$[j]
PRC B-10	$+1.47 \pm 0.16$	···
PRC B-17	$+0.61 \pm 0.06$	$+0.63$[k]
PRC B-19	···	$+1.0$[l]
PRC B-20	$+1.65 \pm 0.10$	···
PRC B-21	$+0.88 \pm 0.04$	$+0.5$[m]
PRC C-02	···	$+0.86$[n]
PRC C-03	···	$+0.9$[o]
PRC C-13	···	$+1.3$[ap]
PRC C-27	···	$+0.6$[n]

[a]Color converted to $B-R$ using the approximate transformations of §4.4. The details of the conversions are mentioned in the notes below.

[b]Reshetnikov et al. (1994), converted from $B-V=+0.55$ obtained in turn by these authors from the $B-g$ and $B-i$ of Whitmore et al. (1990).

[c]Whitmore et al. (1987), converted from $B-V=+0.65 \pm 0.08$.

[d]Peletier & Christodoulou (1993), converted from $B-V=0.71$.

[e]Reshetnikov et al. (1994).

[f]Mould et al. (1982).

[g]Whitmore et al. (1987), converted from $B-V=-0.09$ obtained in turn by these authors from Sérsic & Agüero (1972).

[h]Gallagher et al. (2002), converted from $B-I \approx 1.5$.

[i]Reshetnikov et al. (1994).

[j]Reshetnikov et al. (1995).

[k]Cox et al. (2001).

[l]Arnaboldi et al. (1993).

[m]Reshetnikov et al. (2002).

[n]Reshetnikov (2004).

[o]Reshetnikov et al. (2005).

[p]van Driel et al. (1995), converted from $V-I=1.0$.

5. DISCUSSION

5.1. *Ring Magnitudes*

Our ring magnitudes in R are 1.8 to 4.3 magnitudes fainter than our model magnitudes for the host galaxies. Of course, our ring magnitudes do not include the whole ring. We can make a rough correction to this by assuming that they include half of the ring, in which case the rings are 1.1 to 3.6 magnitudes fainter than the galaxies. Thus, we estimate that these rings contribute between 4% and 40% of the light of the host galaxy, which is in agreement with other authors (approximately 25% in PRC A-05, Gallagher et al. 2002; 11% in PRC C-02, Reshetnikov 2004; 14% for PRC A-04 and 24% for PRC A-06, Reshetnikov & Combes 1994; between 1% and 40% for the confirmed polar-ring galaxies in the PRC, Reshetnikov et al. 1994). The most dominant rings are in PRC A-01 and A-06.

5.2. *Range of Ring Colors*

We have measured the $B-R$ colors of seven polar rings. Previous observers have generally obtained ring colors bluer than $B-R=+1.1$, with the notable exception of van Driel et al. (1995) who obtained $V-I \approx +1.0$ (which suggests $B-R \approx +1.5$) for the ring of PRC C-13 (NGC 660).

Our measured $B-R$ ring colors span a range from $+0.61 \pm 0.06$ to $+1.65 \pm 0.10$. The two reddest rings are PRC B-10 and B-20. In B-10, the ring is faint and the color of $+1.47 \pm 0.16$ is correspondingly uncertain. The color of the ring of B-10 is consistent at the 3σ level with an intermediate color $+1.0$. On the other hand, in B-20 the ring is brighter and has a better measured color of $+1.65 \pm 0.10$, which even with a 3σ departure to the blue would still be as red as $+1.35$. Thus, we consider that B-20 has a truly red ring.

Thus, our work identifies B-20 as a second galaxy with a red ring and confirms that rings have a spread in colors. This spread presumably is caused by differences in one or more of the following: ring ages, metallicities, and internal reddenings.

5.3. *The Blue Rings of PRC B-17 and B-21*

Our two bluest rings, those of PRC B-17 and B-21, are the only ones in our sample that have very bright H II regions (Cox et al. 2001; Watson, unpublished). This suggests that recent star formation is the cause of these blue colors.

5.4. *The Red Ring of PRC B-20*

As we discussed above, the ring of PRC B-20 has a $B-R$ color of $+1.65 \pm 0.10$. A stellar population may show red colors primarily because it is old or because it suffers reddening. Metallicity also modifies the colors, especially for older populations.

Unfortunately, the internal extinction of polar rings is not well understood. Gallagher et al. (2002) formed a color-magnitude diagram for the ring of PRC A-05 on a pixel-to-pixel basis. Dusty pixels were statistically redder and fainter. Unfortunately our data do not have adequate spatial resolution to apply this technique. Furthermore, the technique is insensitive to a uniform extinction.

Additionally, the metallicity of the ring of B-20 is unknown. However, we note that there is distinct absorption from the ring where it passes over the south side of the galaxy. Therefore, it seems unlikely that the ring is especially metal poor. In other rings, the metallicity ranges from about solar (Eskridge & Pogge 1997) to about half solar (Buttiglione, Arnaboldi, & Iodice 2006).

Finally, the transformation between the current colors of a stellar population and its age depend on the detailed star formation history. For example, the ring could have existed for a certain time before it began to form stars. Alternatively, it may have formed stars continuously rather than in a single burst, in which case its colors would be bluer. In our analysis here, we assume that the stars formed in a single burst, which gives a minimum ring age.

We can estimate possible minimum ages for the ring under several different assumptions. We assume the metallicity can range from two-fifths solar ($Z = 0.008$) to solar ($Z = 0.02$) and the internal reddening from 0 to 0.3 magnitudes. An intrinsic color of $+1.65$ would imply a minimum age in excess of 10 Gyr according to the models of Kurth et al. (1999), irrespective of metallicity. On the other hand, an intrinsic color of $+1.35$, arising either from a 3σ departure to the blue or $+0.3$ magnitudes of internal extinction, would imply minimum ages of about 2.5 Gyr for solar metallicity and 5 Gyr for two-fifths solar metallicity. Finally, an intrinsic color of $+1.05$, arising from both 3σ departure to the blue and $+0.3$ magnitudes of internal extinction, would imply minimum ages of about 1.2 Gyr for solar metallicity and 1.7 Gyr for two-fifths solar metallicity.

With a distance of about 140 Mpc (Jones et al. 2004, assuming $H_0 = 75$ km s^{-1} Mpc s^{-1}), the ring diameter of B-20 of about $22''$ corresponds to about 15 kpc. If the orbital velocity at this distance from the galaxy is 120 km s^{-1}, the orbital period is about 0.4 Gyr. If the ring in B-20 is definitely older than 1.2 Gyr, the ring has survived for at least 3 orbital periods and so would appear to be stable.

On the other hand, before we rush to conclude that all polar rings are stable, we must note that the ring in B-20 has not been confirmed as a polar ring; it is simply a good candidate (and, for that matter, neither has the ring in B-10). Confirmation will require measurements of the kinematics of the host galaxy and the ring. Furthermore, our minimum age estimate is severely compromised by uncertainties in the metallicity and internal reddening of the ring. However, future spectroscopy could yield a ring metallicity, and imaging in the near-infrared might reduce the uncertainty due to internal reddening. These observations should be pursued.

We thank Pedro Colín, José Antonio de Diego, Simon Kemp, and Michael Richer for useful comments on an early version of this work. We thank an anonymous referee for a useful report. We are grateful to the staff of the Observatorio Astronómico Nacional on Sierra San Pedro Mártir for their hospitality and technical support during the observing runs. This work has been supported in part by the project IN118302-3 of the UNAM/DGAPA. This research has made use of the NASA/IPAC Extragalactic Database (NED) which is operated by the Jet Propulsion Laboratory, California Institute of Technology, under contract with the National Aeronautics and Space Administration.

REFERENCES

Arnaboldi, M., Capaccioli, M., Cappellaro, E., Held, E. V., & Sparke, L. 1993, A&A, 267, 21
Bournaud, F., & Combes, F. 2003, A&A, 401, 817
Buttiglione, S., Arnaboldi, M., & Iodice, E. 2006, Mem. Soc. Astron. Italiana Suppl., 9, 317
Cox, A. L., & Sparke, L. S. 1996, in ASP Conf. Ser. 106, The Minnesota Lectures on Extragalactic Neutral Hydrogen, ed. Evan D. Skillman (San Francisco: ASP), 168
Cox, A. L., Sparke, L. S., Watson, A. M., & van Moorsel, G. 2001, AJ, 121, 692
Eskridge, P. B., & Pogge, R. W. 1997, ApJ, 486, 259
Gallagher, J. S., et al. 2002, ApJ, 568, 199
Gil de Paz, A., Madore, B. F., & Pevunova, O. 2003, ApJS, 147, 29
Jones, D. H., et al. 2004, MNRAS, 355, 747
Kurth, O. M., Fritze-v. Alvensleben, U., & Fricke, K. J. 1999, A&AS, 138, 19
Landolt, A. U. 1983, AJ, 88, 439L
Lauberts, A., & Valentijn, E. A. 1989, The Surface Photometry Catalogue of the ESO-Uppsala Galaxies (Garching: ESO)
Mould, J., Balick, B., & Aaronson, M. 1982, ApJ, 260, L37
Peletier, R. F., & Christodoulou, D. M. 1993, AJ, 105, 1378
Peletier, R., Davies, R. L., Illingworth, G. D., Davis, L. E., & Cawson, M. 1990, AJ, 100, 1091
Peng, C. Y., Ho, L. C., Impey, C. D., & Rix, H. W. 2002, AJ, 124, 266
Reshetnikov, V. P. 2004, A&A, 416, 889
Reshetnikov, V., Bournaud, F., Combes, F., Fandez-Abans, M., de Oliveira-Abans, M., van Driel, W., & Schneider, S. E. 2005, A&A, 431, 503
Reshetnikov, V. P., & Combes, F. 1994, A&A, 291, 57
Reshetnikov, V. P., Fandez-Abans, M., & de Oliveira-Abans, M. 2002, A&A, 383, 390
Reshetnikov, V. P., Hagen-Thorn, V. A., & Yakovleva, V. A. 1994, A&A, 290, 693
__________. 1995, A&A, 303, 398
Schechter, P. L., & Gunn, J. L. 1978, AJ, 83, 1360
Schlegel, D. J., Finkbeiner, D. P., & Davis, M. 1998, ApJ, 500, 525
Schweizer, F., Whitmore, B. C., & Rubin, V. C. 1983, AJ, 88, 909
Sérsic, J. L., & Agüero, E. L. 1972, Ap&SS, 19, 387
Sparke, L. S. 2004, in High-Velocity Clouds, ed. H. van Woerden, B. P. Wakker, U. J. Schwarz, & K. S. de Boer (Dordrecht: Kluwer), 273
Stockton, A., & MacKenty, J. W. 1983, Nature, 305, 678
van Driel, W., et al. 1995, AJ, 109, 942
Whitmore, B. C., Lucas, R. A., McElroy, D. B., Steiman-Cameron, T. Y., Sackett, P. D., & Olling, R. P. 1990, AJ, 100, 1489
Whitmore, B. C., McElroy, D. B., & Schweizer, F. 1987, AJ, 314, 439

Note added in proof.— In § 4.5 we comment on differences between our photometry of PRC B-21 and that of Reshetnikov et al. (2002). V. Reshetnikov has written to us to point out that PRC-21 has strong color gradients (see, for example, Figure 3 in Reshetnikov et al. 2002) and that our aperture photometry of the central region appears to be in reasonable agreement. Our photometry for the whole galaxy, however, is still significantly different.

A. Godínez-Martínez and A. M. Watson: Centro de Radioastronomía y Astrofísica, Universidad Nacional Autónoma de México, Apdo. Postal 3-72 (Xangari), 58089 Morelia, Michoacán, México (arturogm@gmail.com, a.watson@astrosmo.unam.mx).
L. D. Matthews: Harvard-Smithsonian Center for Astrophysics, Cambridge, MA 02138, USA (lmatthew@cfa.harvard.edu).
L. S. Sparke: Department of Astronomy, University of Wisconsin-Madison, 475 North Charter Street, Madison, WI 53706-1582, USA (sparke@astro.wisc.edu).